An introduction to the control of switching electronic systems☆

Graham C. Goodwin [a,*], David Q. Mayne [b], Keng-Yuan Chen [c], Colin Coates [a], Galina Mirzaeva [a], Daniel E. Quevedo [a]

[a] School of Electrical Engineering and Computer Science, The University of Newcastle, Callaghan, NSW 2308, Australia
[b] Department of Electrical and Electronic Engineering, Imperial College, London, SW7 2BT, England, UK
[c] Department of Electrical and Control Engineering, National Chiao Tung University, Hsinchu, Taiwan

Abstract: Control technology underpins the operation of many, and arguably all, modern high technology systems. Such systems include transportation (aircraft, high speed trains, marine vessels, automobiles), telecommunication systems, electricity networks, mining, minerals processing and agriculture. A particular area where control is playing an increasingly important role is industrial electronics. In this paper we will give a tutorial introduction to the application of control engineering concepts to such systems and reflect on the opportunities and challenges that exist in this area.

1. Introduction

Advanced control is a mature subject. It has gone through various phases of development (Goodwin, Graebe, and Salgado, 1997) including classical control, L_2 optimal control, robust control and, most recently, networked control and quantum control. Often it has been new application areas that have inspired control theory developments. For example, the ideas of network control are responding to the challenges arising from implementing control over a telecommunication network. This problem leads to new questions regarding the impact of limited channel capacity, random delays and lost packets (Goodwin, Quevedo, & Silva, 2008; Silva, Goodwin, & Quevedo, 2010). Also, research in quantum control is inspired by the potential of quantum computing.

A technology that underpins the operation of many modern systems is that of switching electronics. This technology lies at the core of many new systems including smart electricity grids, wind and solar power, high speed trains and electric and hybrid vehicles. These systems give rise to a unique set of control engineering opportunities and challenges. Certainly many of these challenges have already been addressed or are the subject of current research

(Holmes & Lipo, 2003; Kazmierowski, Krishnan, & Blaabjerg, 2002; Mohan, Underland, & Robbins, 1995). In this context, the aim of the current paper is to give a tutorial introduction to the control of power electronics and drives.

An overview of the remainder of the paper is as follows: In Section 2, we briefly review control problems in power electronics and drives. In Section 3, we give a brief overview of basic concepts in control. In Section 4, we illustrate the ideas by reference to the control of a synchronous reluctance machine. In Section 5, we provide a brief overview of model predictive control. In Section 6 we discuss issues involved in providing a "certificate of stability" and we introduce the idea of "fusion control". In Section 7, we discuss challenges and opportunities. Finally, in Section 8, we draw conclusions.

2. Brief overview of control problems in switching electronics

2.1. General comments

In the area of switching electronics, a wide range of circuit topologies are used in various applications. There are many different types of switch mode converter and inverter circuits that find use in power supplies, motor drives and power conditioning applications.

Although the range of circuit architectures is diverse, it is also true that the associated control problems share many common elements. The controllers generally seek to regulate a voltage or current with minimum steady state error while maintaining a fast transient response. In each instance, the controller output is limited to a finite set of values determined by the circuit's switching states. The controller must be robust, remaining

insensitive to variations in plant parameters. For example, the inductance and resistance values in motor drives can vary significantly due to magnetic saturation and thermal effects. Also, one typically wants to minimize excessive switching to enhance efficiency. Finally, allowance must be made for the noise content in feedback signals as power electronic circuits are inherently noisy.

2.2. Motivational example

The torque control of a synchronous reluctance motor (SynRM) Lipo (1991) is used here as a representative problem to demonstrate some of the key control issues in power electronics and drive circuits. The example is also of interest in its own right. Although, the induction motor (IM) is the most popular machine for industrial use, the modern SynRM is considered to be a viable alternative. While providing a torque comparable to that provided by an IM of a similar size, the losses in a SynRM are about 50% of those in an IM. Thus, it is expected that the SynRM will receive increasing attention in the future.

The SynRM is distinguished by its rotor structure where axial laminations, or other techniques, are used to produce both a low reluctance and a high reluctance magnetic flux paths (Matsuo & Lipo, 1994). By convention, the low reluctance axis is called the direct (D) axis and the high reluctance axis is called the quadrature (Q) axis. The stator of a SynRM is typically a three-phase distributed winding as is common to other AC machines. The SynRM develops torque as it seeks to align its low reluctance axis to the stator field.

The control of a SynRM is usually addressed in a rotating DQ reference frame which is fixed to the rotor. This offers the advantage of transforming the AC stator current variables to DC values. Additionally, the transformation removes the position dependence and mutual inductance terms otherwise obtained when operating in stator variables. The voltage and torque equations for a three-phase SynRM in the rotor DQ reference frame are well known (Matsuo & Lipo, 1994):

$$v_d = R_s i_d + L_d \frac{di_d}{dt} - \omega L_q i_q \tag{1}$$

$$v_q = R_s i_q + L_q \frac{di_q}{dt} + \omega L_d i_d \tag{2}$$

$$T = \frac{3}{2}\frac{p}{}(L_d - L_q)i_d i_q \tag{3}$$

Fig. 1 shows the typical control structure for a SynRM drive (Vas, 2003). An outer speed control loop generates a torque reference which translates into the quadrature current reference using (3). Speed in the outer loop can be measured by a sensor (as shown) or estimated using the natural SynRM rotor saliency. The combined direct and quadrature currents are controlled by an inner current control loop that determines the voltage to be applied to the motor in the DQ reference frame. The direct axis current reference is typically set to its rated value. This ensures the machine is fully fluxed and maximum torque is obtained. In a three-phase drive only eight (seven independent) voltage vectors can be applied to the motor via the inverter. The switching selector chooses the most

appropriate voltage vector or sequence of voltage vectors to apply to the machine at each control cycle.

The most common approaches to implementing the current control loop and inverter switching selection blocks are as follows (Cortés, Kazmierowski, Kennel, Quevedo, & Rodríguez, 2008):

(a) *Hysteresis control*: The direct and quadrature current references can be transformed to stator phase current values. These reference values are then compared to the actual stator phase currents. The individual inverter legs are switched to maintain the associated phase current within a band around the reference value (Coates, Platt, & Gosbell, 2001). While this type of controller is simple to implement, it requires higher switching frequencies leading to increased inverter switching losses.

(b) *Linear control with PWM*: The error between the reference and measured values of direct and quadrature currents are fed to respective controllers (typically PI) that generate reference values for the direct and quadrature axis voltages. A pulse width modulator is then used to generate the switching signals for the inverter (Xu, Xu, Lipo, & Novotny, 1991).

(c) *Predictive control methods*: Given the measured state of the machine, the motor voltage equations can be used to determine the ideal direct and quadrature voltages to move the current vector to its desired value in one step. In this instance, the switching selector chooses the inverter switching configuration (or a combination of switching configurations) that is closest to approximating the ideal voltage vector. This switching configuration is applied over the next control cycle, (Coates et al., 2001; Cortés et al., 2008).

(d) *Other control techniques* Various other strategies including fuzzy logic and sliding mode have also been applied in this area.

We will use a multi-degree-of-freedom control architecture in Section 4 for a nine-phase SynRM to illustrate basic ideas in this area.

3. A tutorial overview of basic control concepts

3.1. Inversion

At a high level of abstraction, we can view the problem of control as one of inversion (Goodwin et al., 1997). One has a system – usually called the "plant" – which has outputs – process variables. The plant is acted upon by inputs (manipulated variables). The core problem is to choose the inputs so that the outputs achieve certain objectives. If one has a model linking inputs to outputs, then one sees that the above problem can, in principle, be solved by inverting the model so as to evaluate the necessary inputs which bring the outputs to their desired values. Thus, conceptually, if the model takes the form:
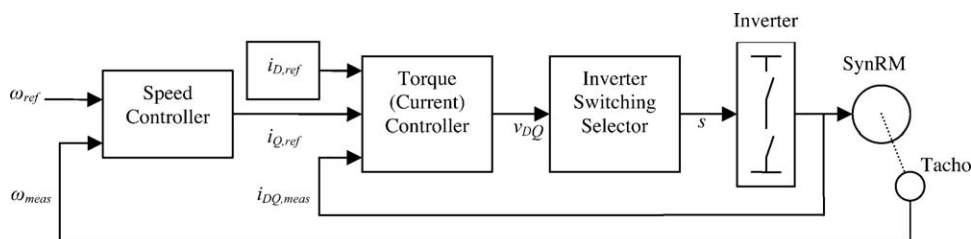
$$y = G(u) \tag{4}$$

Fig. 1. Synchronous reluctance motor drive

where y, u denote the output and input respectively, and we want y to be y^*, then the required input is simply given by:

$$u^* = G^{-1}(y^*) \tag{5}$$

Of course, there are a number of practical issues which render this solution too naive in most real situations. Some of the additional features of real problems include (Goodwin et al., 1997):

(i) *Disturbances*: The output response y is influenced by (load) disturbances in addition to the input, u.

(ii) *Measurement errors*: It is helpful, at least intuitively, to know if y has reached the target value y^*. However, the measurements of y are typically corrupted by noise and other measurement imperfections.

(iii) *Input constraints*: It is usual that we cannot apply desired inputs to the plant. For example, in switching electronics, the input will typically be restricted by the finite set of available switch positions. Thus one must "make the best use of" the available input options.

(iv) *Dynamics*: The model (4) implies that the effect of changing the input is instantaneous on the output. However, all real systems are subject to energy storage and delays, i.e., the voltage in capacitors and the current in conductors cannot be changed instantly.

(v) *Model errors*: Typically the model $G(\cdot)$ is, at best, only approximately known. Hence one needs to find a way of obtaining an inverse which is insensitive to model errors.

(vi) *Time Variations*: Typically the model $G(\cdot)$ will not be fixed, e.g., resistor and inductor values can change as the temperature changes.

(vii) *Robustness*: This is a term used to describe control systems that operate satisfactorily in the light of the kind of problems mentioned under (v) and (vi) above.

In the sequel we will use a slightly more general way of modelling the system. We will use a transfer function description based on z-transforms:

$$y(z) = G(z)u(z) + d_0(z) \tag{6}$$

$$y_m(z) = y(z) + n(z) \tag{7}$$

where n, d_0 represent (the z-transform of) measurement noise and process disturbances (lumped at the output). (The z-transform variable can also be interpreted as the forward shift operator thus giving a direct mechanism for implementing the required control law transfer functions.)

3.2. High gain feedback

It turns out that a remarkably robust way of achieving "inversion" is via feedback. Thus, if we have a desired value, y^*, for y, then we might envisage generating the input via a feedback law of the form:

$$u(z) = -C(z)y_m(z) + M'(z)y^*(z) \tag{8}$$

To simplify developments we will temporarily restrict attention to single-input single-output systems. (The results apply more generally.) Also, for the moment, we choose $M'(z) = C(z)$. (Other choices will be explored in Section 3.6).

Solving (6)–(8) simultaneously gives the following "closed loop" relationship:

$$y(z) = \frac{G(z)C(z)}{1 + G(z)C(z)}y^*(z) - \frac{G(z)C(z)}{1 + G(z)C(z)}n(z)$$
$$+ \frac{1}{1 + G(z)C(z)}d_0(z) \tag{9}$$

Eq. (9) motivates us to introduce the two key closed loop transfer functions $T(z)$ and $S(z)$. These are called the complementary sensitivity and sensitivity, respectively:

$$T(z) = \frac{G(z)C(z)}{1 + G(z)C(z)} \tag{10}$$

$$S(z) = \frac{1}{1 + G(z)C(z)} \tag{11}$$

We can then write

$$y(z) = T(z)y^*(z) - T(z)n(z) + S(z)d_0(z) \tag{12}$$

We now see how feedback is a way of achieving inversion. All we need to do is make $C(z)$ "very large" to achieve:

$$T(z) = 1 \tag{13}$$

In this case, the "closed loop" transfer function from y^* to y becomes 1 and $u(z) = G(z)^{-1}[y^*(z) - d_0(z)]$ as required.

3.3. Design trade-offs

Alas, the above (high gain) solution to the control problem is not as easy as it sounds. For example, Eq. (9) shows that putting $T(z) = 1$, causes the measurement noise to be transferred to the output $y(z)$. Another slightly more subtle issue is that we see from Eqs. (10) and (11) that

$$T(z) + S(z) = 1 \tag{14}$$

Hence, if we want low sensitivity to measurement noise ($T(z) \rightarrow 0$), then necessarily we have 100% sensitivity to (output) disturbances ($S(z) \rightarrow 1$), and vice versa.

Actually, there is another reason why we may not want to have infinite (or a least very high) gain in the controller. The reason is that we usually only have an approximate model. To illustrate, let us describe model errors in the frequency domain by saying that the *true* plant transfer function, $G(z)$ is related to the given model, $G_0(z)$, by a relationship of the form:

$$G(e^{j\omega\Delta_s}) = G_0(e^{j\omega\Delta_s})\left[1 + G_\Delta(e^{j\omega\Delta_s})\right] \tag{15}$$

where Δ_s is the sampling period.

We say that $G_\Delta(e^{j\omega\Delta_s})$ is the multiplicative error at frequency ω.

One can then easily derive the following relationship between the true sensitivity function $S(e^{j\omega\Delta_s})$ and the nominal sensitivity function $S_0(e^{j\omega\Delta_s})$:

$$S_0(e^{j\omega\Delta_s}) = \frac{1}{1 + G_0(e^{j\omega\Delta_s})C(e^{j\omega\Delta_s})} \tag{16}$$

$$S(e^{j\omega\Delta_s}) = \frac{S_0(e^{j\omega\Delta_s})}{1 + T_0(e^{j\omega\Delta_s})G_\Delta(e^{j\omega\Delta_s})} \tag{17}$$

Say one designs $S_0(e^{j\omega\Delta_s})$ to be small (over some frequency range), then $T_0(e^{j\omega\Delta_s})$ will be near unity over the same frequency range. Thus we see that there is a potential danger arising from $G_\Delta(e^{j\omega\Delta_s})$. Indeed, a sufficient condition for closed loop stability is that $|T_0(e^{j\omega\Delta_s})||G_\Delta(e^{j\omega\Delta_s})|$ should be less than 1 at all frequencies. This is a simple consequence of (17).

Usually, in practical models, $|G_\Delta(e^{j\omega\Delta_s})|$ is large at high frequency. Thus robustness to model errors typically places an upper band on the frequencies over which $|T_0(e^{j\omega\Delta_s})|$ can be kept near 1. In practice, one usually makes $S(z)$ identically zero (i.e., $T(z) = 1$) at dc by including an integrator in the controller (i.e., a pole at $z = 1$). Then one designs $C(z)$ so that $S(z)$ to approaches 1 at some higher frequency. We call the resultant range of frequencies where $S(z) < 1$ the "closed loop bandwidth".

There are other reasons why one cannot make $S_0(e^{j\omega\Delta_s})$ small at *all* frequencies. These constraints arise from the need to keep $S_0(e^{j\omega\Delta_s})$ stable, i.e., to keep $S_0(z)$ an analytic function. In a key result, Bode showed that for all analytic functions, we have (Goodwin et al., 1997)

$$\int_{-\pi/\Delta_s}^{\pi/\Delta_s} \log|S_0(e^{j\omega\Delta_s})|d\omega \geq 0 \tag{18}$$

Of course, $\log|a| \geq 0$ if $a \geq 1$. Hence, (18) tells us that there is a remarkable "water bed" effect, i.e., if we have a range of frequencies where $|S_0(e^{j\omega\Delta_s})| < 1$, then there must be another range of frequencies where $|S_0(e^{j\omega\Delta_s})| > 1$.

3.4. State estimate feedback

In modern control it is common to replace the transfer function model of (6) by a state variable model of the form:

$$x^+ = Ax + Bu \tag{19}$$

$$y = Cx \tag{20}$$

where x^+ is the next value of x.

If the state was directly measured, then one could design static state variable feedback of the form:

$$u = -Kx + M(z)y^* \tag{21}$$

Subject to mild assumptions (e.g., controllability) then K can be chosen to give desired closed loop properties. (e.g., a specified closed loop bandwidth.)

However, x is not usually directly measured. In this case one can obtain an estimate of x by using an observer:

$$\hat{x}^+ = A\hat{x} + Bu + J(y - C\hat{x}) \tag{22}$$

where J is so chosen that $(A–JC)$ is stable, and implement the control law as:

$$u = -K\hat{x} + M(z)y^* \tag{23}$$

We can actually reinterpret the controller given in (22) and (23) in the Classical Transfer Function form as in Sections 3.2 and 3.3 by taking z-transforms in (22). This leads to

$$u = -T_1(z)u - T_2(z)y + M(z)y^* \tag{24}$$

where

$$T_1(z) = K(zI - A + JC)^{-1}B =: \frac{R(z)}{E(z)} \tag{25}$$

$$T_2(z) = K(zI - A + JC)^{-1}J =: \frac{P(z)}{E(z)} \tag{26}$$

Rearranging (24) we obtain:

$$u = -C(z)y + M'(z)y^* \tag{27}$$

where $C(z) = P(z)/[R(z) + E(z)] =: P(z)/L(z)$; $M'(z) := E(z)M(z)/L(z)$.

Thus we have given a modern interpretation (in the form of state estimate feedback) to the classical control law given in (8).

3.5. Internal models

An important practical issue when designing feedback control laws is to ensure that certain disturbances are exactly cancelled at the output. We can achieve this goal by including a model for the disturbances in the description (19).

To explain this idea in more detail, say that we have an input disturbance d_i. We can model d_i as the output of a state space

model as shown in (28). The true input to the plant is $u + d_i$.

$$x_d^+ = A_d x_d \tag{28}$$

$$d_i = C_d x_d \tag{29}$$

Common choices for A_d would be a scalar matrix consisting of unity (to describe a constant disturbance) or 2 dimensional matrix having eigenvalues on the unit disc (to describe a sinusoidal disturbance of a given frequency).

The system matrices for the observer and associated feedback control law then take the form:

$$A = \begin{bmatrix} A_0 & B_0C_d \\ 0 & A_d \end{bmatrix}; \quad B = \begin{bmatrix} B_0 \\ 0 \end{bmatrix} \tag{30}$$

$$J = \begin{pmatrix} J_0 \\ J_d \end{pmatrix}; \quad C = [C_0 \quad 0] \tag{31}$$

$$K = [K_0 \quad C_d] \tag{32}$$

Notice that this control law cancels the *estimated* disturbance at the input.

It can readily be shown that, in this case, $L(z) = R(z) + E(z)$ is given by:

$$\begin{aligned} L(z) &= det[zI - A + JC + BK] \\ &= det\begin{bmatrix} zI - A_0 + J_0C_0 + B_0K_0 & -B_0C_d + B_0C_d \\ J_dC_0 & zI - A_d \end{bmatrix} \\ &= det\begin{bmatrix} zI - A_0 + J_0C_0 + B_0K_0 & 0 \\ J_dC_0 & zI - A_d \end{bmatrix} \\ &= det(zI - A_d)det(zI - A_0 + J_0C_0 + B_0K_0) \end{aligned} \tag{33}$$

Hence we conclude that $L(z)$ will be zero at the zeros of the disturbance model. In particular, we obtain an integrating control law if we model the disturbance as containing an (unknown) constant.

The significance of this observation will be made clear in the next section.

3.6. Multi-degree-of-freedom control laws

The operation of a feedback control loop typically needs to deal with multiple (and often conflicting) design objectives. For example:

(a) We may want to minimize the impact of (unmeasured) load disturbances on the output. (This is governed by $S(z) = 1/[1 + G(z)C(z)]$.)
(b) We may want to minimize the impact of measurement noise on the output. (This is governed by $T(z) = G(z)C(z)/[1 + G(z)C(z)]$.)
(c) We may want to track a given reference signal y^*. (Also, y^* will typically be time varying.)
(d) We may want to minimize the impact of implementation errors (e.g., quantization) in $u(t)$ on the output.

3.6.1. Disturbances and noise

The situation regarding points (a) and (b) is fundamentally constrained by the fact that

$$S(z) + T(z) = 1 \tag{34}$$

The linking of goals (a) and (b) is inescapable since the relevant part of the control law only uses the measurement y, i.e., it has only one-degree-of-freedom, namely $C(z)$.

The situation regarding points (b) and (c) is different because we have extra measurements that we can exploit.

3.6.2. Reference feedforward

We use feedforward to give an extra degree-of-freedom. Indeed, this has already been included in the control law in (24) and (27) via the transfer function $M(z)$. A typical choice for $M(z)$ is

$$M(z) = \frac{P(z)}{E(z)} + \frac{L(z)}{E(z)} F(z) \qquad (35)$$

or, equivalently, $M'(z) = C(z) + F(z)$.

The resultant transfer function from y^* to y now becomes

$$T_{y^*y}(z) = 1 - \frac{L(z)[A(z) - F(z)B(z)]}{A(z)L(z) + B(z)P(z)} \qquad (36)$$

We also recall the transfer function from d_0 to y which is

$$S_{d_0y}(z) = \frac{A(z)L(z)}{A(z)L(z) + B(z)P(z)} \qquad (37)$$

Examination of (36) and (37) reinforces the importance of the result derived earlier in (33), namely provided (28) and (29) include a model for the disturbance and the reference, then perfect tracking is obtained *irrespective of model errors* since $L(z_0) = 0$, where z_0 is a zero of the disturbance (and reference) model.

We also see the advantages of having $F(z)$ in (36), namely we can reduce the tracking error at every frequency where $F(z)$ can be chosen as an approximate inverse to the plant at these frequencies, i.e.,

$$F(z) \simeq \left[\frac{B(z)}{A(z)}\right]^{-1}; \quad z = e^{j\omega\Delta_s} \qquad (38)$$

The transfer function $F(z)$ provides feedforward control from the measured reference signal.

3.6.3. Input imperfections

We next turn to point (d). This issue is of great importance in switching electronics since the switched nature of the input restricts the allowed input to a finite set. We can describe this implementation "defect" via

$$u(t) = Q[u_0(t)] \qquad (39)$$

where $u(t) \in \mathbb{U}$ (the allowable set), $u_0(t)$ is the desired input coming from the controller and Q is a nonlinear mapping (a generalized "quantizer" Gersho & Gray, 1992).

For design purposes, it is often helpful to think of the difference between $u_0(t)$ and $Q(u_0(t))$ as a noise source, $q(t)$, where

$$q(t) = Q(u_0(t)) - u_0(t) \qquad (40)$$

or

$$u(t) = u_0(t) + q(t) \qquad (41)$$

We could rely upon the feedback controller, $C(z)$, to reduce the impact of q on the output. However, this may compromise the design relative to the impact of d_0 and n. Hence, we introduce an extra degree-of-freedom by introducing another feedforward term via a transfer function $H(z)$ from the measured disturbance $q(t)$. This leads to the, so called, *feedback quantizer* shown in Fig. 2.

If we model the quantizer as a noise source as in (41), then with $H(z) = 0$, we see that the local transfer function from $q(t)$ to $u(t)$ is 1.

On the other hand, if we introduce the additional transfer function $H(z)$ then the transfer function from $q(t)$ to $u(t)$ becomes $1 - H(z)$. Hence, we can choose $H(z)$ to "shape" the frequency content of the errors due to the quantizer. Most importantly, this can be achieved without compromising or affecting any of the other design objectives.

To illustrate, say we implement the controller digitally and we want to eliminate errors *due to the quantizer* at ω_0.
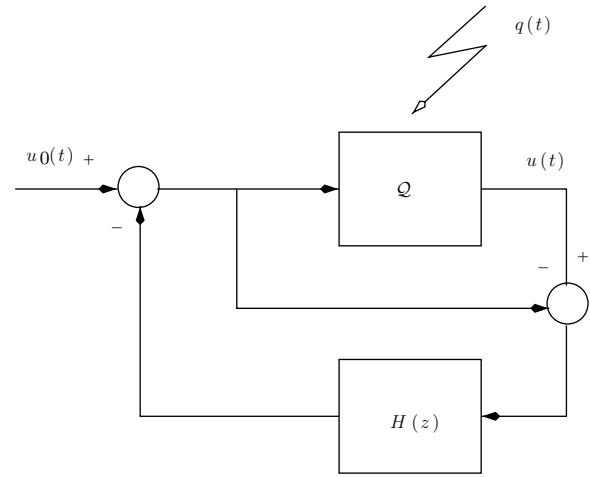

Fig. 2. Feedback quantizer

Then we can choose

$$H(z) = \frac{[2(1-\alpha)\cos\omega_0\Delta_s]z + (\alpha^2 - 1)}{z^2 - (2\alpha\cos\omega_0\Delta_s)z + \alpha^2} \qquad (42)$$

This leads to

$$1 - H(z) = \frac{z^2 - (2\cos\omega_0\Delta_s)z + 1}{z^2 - (2\alpha\cos\omega_0\Delta_s)z + \alpha^2} \qquad (43)$$

This transfer function is zero at frequency $\omega = \omega_0$.

The effectiveness of this strategy in eliminating unwanted components arising from a quantizer is illustrated by the following example. We simulate a feedback control loop for a first order plant with integral action in the controller. We first use a simple (nearest neighbour) quantizer. Fig. 3 shows the spectrum of the input signal in this case. It can be seen that there is a significant spectral peak near 45 Hz arising from "quantization noise". This might have undesirable practical consequences, e.g., it may excite a resonance in a motor. When we introduce an extra degree-of-freedom, via the filter $H(z)$ (see (42)) in the quantizer, then as shown in Fig. 4, the unwanted spectral line disappears. Of course, the Bode integral (18) also holds for $S'(z) = 1 - H(z)$. This implies that there must be a trade-off, i.e., reduction of "quantization noise" at one frequency must be accompanied by an increase in "quantization noise" at other frequencies. This effect is also evident in Figs. 3 and 4. This idea can be used to eliminate (or at least reduce) any undesirable frequency component on the input (subject to satisfaction of the Bode integral trade-off).
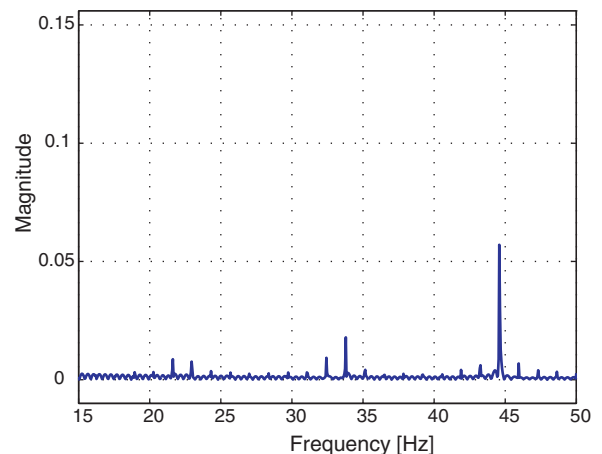

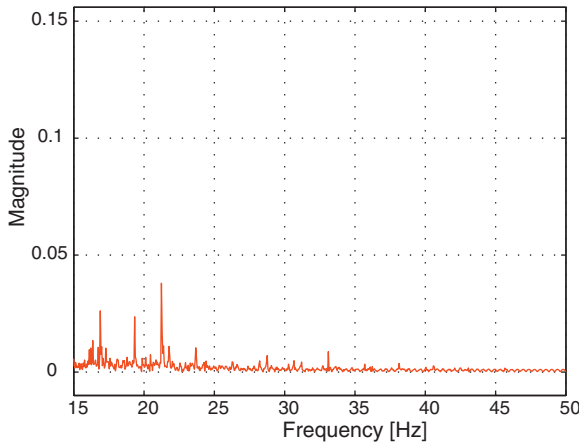Fig. 3. Input spectrum using nearest neighbour quantizer

Fig. 4. Input spectrum using feedback quantizer

3.7. Constrained observer feedback (COF)

A final problem that we wish to discuss is that of input saturation. Specifically, a high gain linear feedback law is almost certain to call for larger inputs (e.g., voltages) than are available. This problem is central to many practical control problems including switching electronics.

A key approach to dealing with these problems is to make sure that the various controllers are "informed" that the (hypothetical) input requested by the linear control law was not actually used. This concept turns out to be a (mild) generalization of well known ideas used in integral control to prevent integrator wind up. These techniques are usually called Anti-Wind-Up (AWU) Control (Goodwin et al., 1997).

We discuss this issue below for the feedback controller, $C(z) = P(z)/L(z)$, and the feedforward controller, $F(z)$.

3.7.1. Feedback controller

In this case, the solution is rather simple. All we need to do is to ensure that the observer part of the feedback controller "knows" about the true input rather than the hypothetical input generated by the linear controller.

Hence the appropriate circuit is as shown in Fig. 5.

3.7.2. Feedforward controller

The situation with feedforward control is a little more subtle. To deal with this, we factor $F(z)^{-1}$ as follows:

$$F(z)^{-1} = f_0 + \bar{F}(z) \tag{44}$$

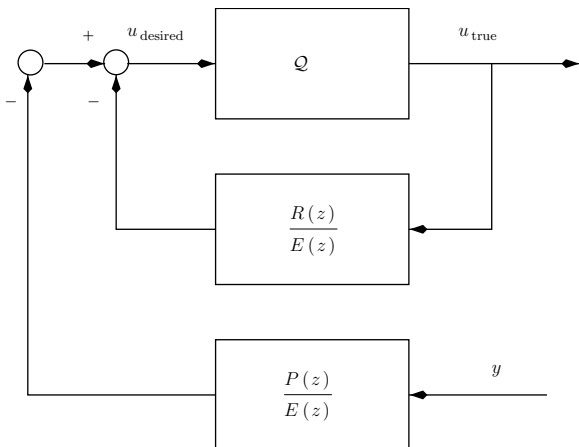where $\bar{F}(z)$ is strictly proper.

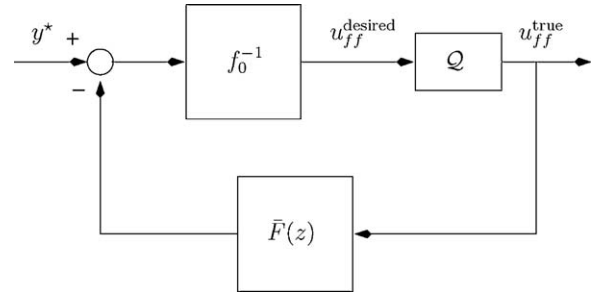**Fig. 5.** COF implementation of feedback controller

Fig. 6. COF implementation of feedforward controller

We then implement the feedforward controller as shown Fig. 6. We see that, in the absence of quantization, or saturation, that

$$u_{ff}^{\text{true}} = \frac{f_0^{-1}}{1 + f_0^{-1}\bar{F}(z)} y^* = F(z)y^* \text{ as required} \tag{45}$$

However, in the presence of quantization, the circuit ensures that the states of the feedforward filter which appear in $\bar{F}(z)$, "know" that u_{ff}^{true} was actually used rather than u_{ff}^{desired}.

3.8. Composite design

Finally, we can put all of the elements together. One final point to be addressed is that u comprises two signals, i.e., u_{ff} and u_{fb}.

Hence we define

$$\lambda = \left| \frac{Q\left[u_{ff}^{\text{desired}} + u_{fb}^{\text{desired}}\right]}{\left[u_{ff}^{\text{desired}} + u_{fb}^{\text{desired}}\right]} \right| \tag{46}$$

Then we calculated

$$\begin{aligned} u_{ff}^{\text{actual}} &= \lambda u_{ff}^{\text{desired}} \\ u_{fb}^{\text{actual}} &= \lambda u_{fb}^{\text{desired}} \end{aligned} \tag{47}$$

We can then draw the complete design as in Fig. 7.

4. Illustration via control of synchronous reluctance motor

To illustrate some of the ideas described above we will present results for the (simulated) control of a nine-phase voltage source inverter driving a SynRM – see Fig. 8 and Section 2. We will focus on torque control with constant fluxing of the machine.

We will investigate the impact of the design and implementation (in COF form) of the feedback and feedforward loops. We use a sample period of $\Delta_s = 0.2$ ms.

4.1. The feedback controller

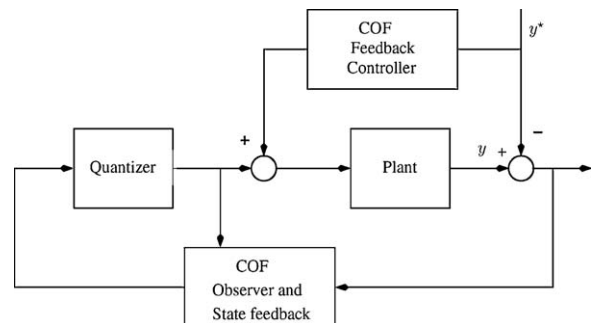For simplicity, we examine the locked rotor scenario. Comments on the non-locked case will be given in Section 6.4. We

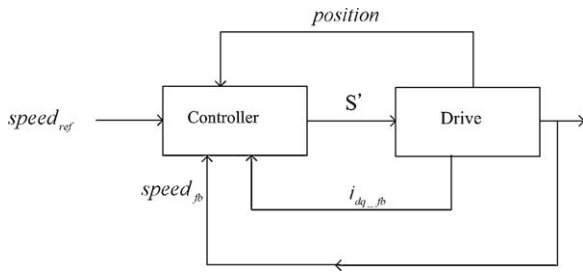**Fig. 7.** COF implementation of complete control law

Fig. 8. SynRM control

Fig. 11. Mean square error as a function of closed loop bandwidth

assume a constant direct axis reference current of 2(A) and we measure all currents in the presence of measurement noise. Hence, in view of the comments made under headings (a) and (b) in Section 3.6, we will need to limit the feedback bandwidth so as to obtain an appropriate trade-off between disturbance rejection and noise immunity.

We utilize a simple PI controller where we cancel the (stable) plant pole by a zero in the controller and introduce integral action. This leads to:

$$C(z) = \frac{K_p(z-1) + K_I \Delta_s z}{(z-1)} \tag{48}$$

where $K_I = (1+\gamma)(1-\alpha)/[\Delta_s \beta]$; $K_p = \alpha(1-\gamma)/\beta$, where α is the open loop (discrete time) pole, γ is the desired (discrete time) closed loop pole.

We implement the controller in COF form as shown in Fig. 9 where $C(z)^{-1} = c_0 + \bar{C}(z)$, $c_0^{-1} = (K_p + K_I \Delta_s)$, and where the quantizer is placed immediately after c_0^{-1}.

The quantizer is a mechanism which ensures that the voltage corresponds to one of the allowed switching states.

We simulate the measurement noise as uniformly distributed white noise in the interval $[-0.1, 0.1]$. We then use this to give about 10% measurement noise as shown in Fig. 10.

Fig. 11 shows the mean square torque error as a function of closed loop bandwidth. As we increase the bandwidth the effect of disturbances decreases but the effect of measurement noise increases. Thus there is an optimal trade-off. We see from Fig. 11 that the optimal closed loop bandwidth is approximately 200 Hz.

Next we vary the noise amplitude and plot the optimum bandwidth as a function of noise amplitude. The results are shown
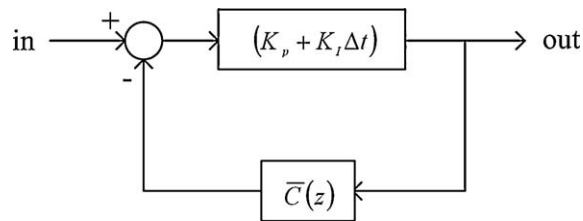

Fig. 12. Optimum bandwidth as a function of measurement noise amplitude

in Fig. 12. As expected, the optimum bandwidth decreases as we increase the measurement noise level.

Finally, we test the use of COF feedforward. We design the (unconstrained) response time of the feedforward to be 1/5th that of the feedback loop. We use a set point change of 10% downwards after reaching steady state. (We choose a small reference change so that the results are not dominated by input slewing resulting from saturation effects.)

Fig. 13 compares the measured response time for 3 controllers as follows:

(i) TFV – this is the predictive control method described in part (b) of Section 2.
(ii) PI controller (in feedback COF form).
(iii) PI controller with compensator (feedback and feedforward controller in COF form).

We see from Fig. 13 that controller (iii) gives approximately 50% reduction in closed loop transient time *independent* of the closed loop bandwidth.

Fig. 9. COF implementation of feedback controller

Fig. 10. Measurement noise generation

Fig. 13. Response times achieved with different control laws
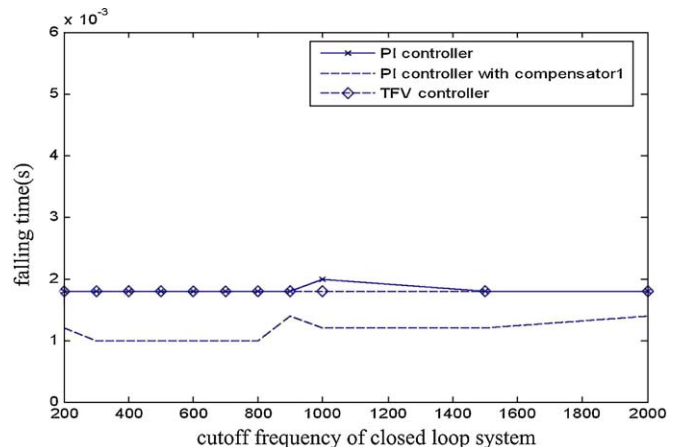
5. A brief introduction to model predictive control

5.1. Overview

Model predictive control (MPC) (Camacho and Bordons, 1999; Goodwin, Serón, & De Doná, 2005; Maciejowski, 2002; Rawlings & Mayne, 2009) has emerged as a very successful method to solve a wide range of problems in the process industries where the plant being controlled is "slow" (Qin & Badgwell, 2003). The method is being increasingly employed to control "fast" plants including switching electronics Kouro et al. (2009), Linder and Kennel (2005), Rodríguez et al. (2007), Vargas et al. (2007), Lezana et al. (2009), Huang and Corzine (2006), Cortés et al. (2008), Cortés et al. (2009), Aguilera et al. (2008). Here the sampling rate is high (<1 ms) and hence special attention must be placed on computational issues. MPC owes its success to its ability to (relatively easily) handle nonlinearity of the plant and to allow one to impose hard constraints on states and controls. These are requirements that are difficult to satisfy with other control methods. The penalty is that an open-loop optimal control problem (possibly nonlinear and constrained) has to be solved at each instant to obtain the control.

5.2. Basic ingredients of deterministic MPC

To allow for consideration of nonlinear systems, suppose the plant to be controlled is described by

$$x^+ = f(x, u) \tag{49}$$

where x and u denote, respectively, the state and control, and x^+ denotes the successor state, i.e., the state at the next sampling instant. Suppose the length of the horizon of the optimal control problem to be solved is N and that the plant is subject to the control (input) constraint $u \in \mathbb{U}$ and state constraint $x \in \mathbb{X}$. We discuss the deterministic case. By "deterministic" we imply that there is no uncertainty in the system. In particular, the state x is assumed to be known and there are no unknown disturbances. The optimal control problem (solved on line) requires that, for the known current state x at time t, a constrained minimization be carried out with respect to the control sequence $\mathbf{u} = \{u(0), u(1), \ldots, u(N-1)\}$. Because the system is time-invariant, it is convenient to regard the initial time in the optimization problem to be 0. The state at each time $k > 0$ is a function of $(x, \mathbf{u})$. Hence, the cost $V_N(\cdot)$ is defined by

$$V_N(x, \mathbf{u}) := \sum_{i=0}^{N-1} \ell(x(i), u(i)) + V_f(x(N)) \tag{50}$$

in which $x(i) = \phi(i; x, \mathbf{u})$ is the solution at time i of the difference equation $x^+ = f(x, u)$ when the initial state is x and the control (input) sequence is chosen as $\mathbf{u}$. The minimization is carried out subject to the control and state constraints $u(i) \in \mathbb{U}$ and $x(i) \in \mathbb{X}$ for all $i \in \{0, 1, 2, \ldots, N-1\}$. It is also usual to impose a terminal state constraint of the form $x(N) \in X_f$. In this formulation, $V_f(\cdot)$ is the additional terminal cost (a Control Lyapunov Function in the neighbourhood of the set point) and $X_f \subseteq \mathbb{X}$ is the associated control positive invariant set. (A discussion of control Lyapunov functions can be found in Rawlings and Mayne (2009)). These are added to the optimal control problem as a mechanism to provide a certificate of stability. The minimization yields the optimal control sequence

$$\mathbf{u}^0(x) = \{u^0(0; x), u^0(1; x), \ldots, u_{N-1}(0; x)\} \tag{51}$$

This is a function of the current state x as well as the value function $V_N^0(x) = V_N(x, \mathbf{u}^0(x))$. Model predictive control implements the solution in a "rolling horizon" fashion, i.e., we use only $u^0(0; x)$, the first element of this sequence, as the control u to be applied to the plant. The control $u = \kappa_N(x) := u^0(0; x)$ applied to the plant is a function of the state. Hence a particular form of static (nonlinear)

state feedback control is obtained. When time advances one step, we measure (or estimate) the current state and repeat the calculation.

5.3. Stability

Subject to conditions on $f(\cdot)$, $\ell(\cdot)$, $V_f(\cdot)$ and X_f, then closed-loop stability (i.e., asymptotic or exponential) can be established (Mayne, Rawlings, Rao, & Scokaert, 2000) for the closed-loop system $x^+ = f(x, \kappa_N(x))$. This result is obtained using the value function $V_N^0(\cdot)$ as a Lyapunov function. Satisfaction of the conditions mentioned above ensures $V_N^0(\cdot)$ is zero at the target state, positive elsewhere and satisfies:

$$V_N^0(x^+) \leq V_N^0(x) - \ell(x, \kappa_N(x)), \quad x^+ = f(x, \kappa_N(x)) \tag{52}$$

Thus $V_N^0(\cdot)$ decreases along closed-loop trajectories and this ensures closed-loop stability. The analysis also shows that recursive feasibility is maintained, i.e., if the optimal control problem can be solved at the initial time, it can be solved at all future times. If the terminal cost is chosen appropriately (this is easy when the system is linear) and the set of states to be controlled restricted to a region around the target state, performance is identical to that obtained using an infinite horizon optimal control problem.

5.4. Nonconvex problems

If, the optimal control problem is non-convex (which is often the case if $f(\cdot)$ is nonlinear), then finding the global minimum of $V_N(\cdot)$ is problematic. However, it has been shown (Rawlings & Mayne, 2009) that determining, at each time, a feasible, rather than an optimal, solution yields, under mild conditions, a stabilising controller. Moreover, recursive determination of a feasible solution is always possible if the initial problem is feasible.

5.5. Specialization to linear systems with quadratic cost

5.5.1. Formulation
Here we study the special case where the system $f(\cdot)$ is linear as in (19) and (20) and the cost is quadratic.

Say that the current state estimate is $\hat{x}(0)$, then the future states over horizon N can be predicted via:

$$\hat{\hat{x}}(i) = A^i \hat{x}(0) + \sum_{k=1}^{i} A^{i-k} B u(k - i + 1) \tag{53}$$

where $i = 1, \ldots, N$. (Note that here we do not include a terminal cost.)

Let us assume a simple cost function of the form:

$$V_N(\hat{x}(0), \mathbf{u}) = \sum_{k=1}^{N} \hat{\hat{e}}^2(k) + \lambda u^2(k-1) \tag{54}$$

where $\hat{\hat{e}}(k) = C\hat{\hat{x}}(k)$. Clearly this is a quadratic function of $\hat{x}(0)$ and $\mathbf{u} = \{u(0), u(1), \ldots, u(N-1)\}$.

Now the cost function (54) can be expressed in matrix notation as:

$$V_N(\hat{x}(0), \mathbf{u}) = (\mathcal{H}\mathbf{u} + \mathbf{r})^T(\mathcal{H}\mathbf{u} + \mathbf{r}) + \lambda \mathbf{u}^T \mathbf{u} \tag{55}$$

where

$$\mathcal{H} = \begin{bmatrix} CB & & 0 \\ & \ddots & \\ CA^{N-1}B & \cdots & CB \end{bmatrix} \tag{56}$$

$$\mathbf{u} = \begin{bmatrix} u(0) \\ \vdots \\ u(N-1) \end{bmatrix}; \mathbf{r} = \begin{bmatrix} CA \\ \vdots \\ CA^N \end{bmatrix} \hat{x}(0) \tag{57}$$

$\mathcal{H}$ contains the system Markov parameters and r is the extended observability matrix.

5.5.2. Unconstrained solution

In the absence of constraints, we can easily find **u** that minimizes (55) namely

$$\mathbf{u} = -\left[\mathcal{H}^T\mathcal{H} + \lambda I\right]^{-1}\mathcal{H}^T\mathbf{r} \tag{58}$$

5.5.3. Constrained solution

In the presence of constraints, we need to minimize (55) subject to satisfaction of the constraints.

When rolling horizon optimization is used, we implement $u(0)$ only. We then measure (or estimate) a new state $\hat{x}(1)$, reset the current time to zero and repeat the problem. At each step, we apply:

$$u(0) = [1 \quad 0 \quad \dots \quad 0]\mathbf{u}^* \tag{59}$$

where $\mathbf{u}^*$ is the vector optimizing the cost function.

5.5.4. Horizon 1

In many applications (including switching electronics) the sampling rate is often very high (e.g. Δ_s is typically chosen as a fraction of a millisecond). In this case, it is usually prohibitive to use large values for the horizon N. Hence it is common to use small horizons, e.g., unity.

When there are no constraints, then it can be seen, by specializing (58) to horizon 1, that the input is given by:

$$u(0) = -K\hat{x}(0) \tag{60}$$

where, in this special case,

$$K = \left[B^TC^TCB + \lambda I\right]^{-1}CBCA.$$

When constraints are added, it is relatively simple to modify the solution as shown below. Let $u^{uc}(0)$ be the solution to the unconstrained problem. Then the cost can be factored as:

$$V_N(\hat{x}(0), \mathbf{u}) = [u(0) - u^{uc}(0)]^T\left[B^TC^TCB + \lambda I\right][u(0) - u^{uc}(0)]$$
$$+ \text{constant} \tag{61}$$

Next say that we require that $u(0) \in \mathbb{U}$, a given constraint set. (Note that this set can be convex or finite.)

We factor the Hessian in the above expression as follows:

$$D^TD = \left[B^TC^TCB + \lambda I\right] \tag{62}$$

and define

$$\bar{u} = Du(0)$$
$$\bar{u}^{uc} = Du^{uc}(0)$$

We also transform the allowable constraint set by defining

$$\bar{\mathbb{U}} = D\mathbb{U} \tag{63}$$

Then we see that

$$V_N(\hat{x}(0), \mathbf{u}) = (\bar{u} - \bar{u}^{uc})^T(\bar{u} - \bar{u}^{uc}) + \text{constant} \tag{64}$$

We also see that the constrained optimization problem is solved by finding the closest value (in a Euclidean sense) within $\bar{\mathbb{U}}$ to the unconstrained solution $\bar{u}^{uc}$.

In summary, we have that the constrained optimal solution is

$$u(0) = D^{-1}\left[\overline{Q}\{Du^{uc}(0)\}\right] = Q[u^{uc}(0)] \tag{65}$$

where $\overline{Q}$ and Q denote a simple "nearest neighbour" quantizer and a generalized quantizer respectively.

We thus see that the horizon 1 solution is defined via the generalized "projection" quantizer given in (65). Moreover, it is clear that the horizon 1 solution is a special case of the COF principle described in Section 3.7 where the "quantizer" takes the form given in (65). For this reason, using the term MPC in this context is perhaps misleading. We thus prefer the term "COF" rather than "MPC" for the horizon 1 case, see (Goodwin, Quevedo, and McGrath (2003), Quevedo and Goodwin (2005), De Doná, Goodwin, and Serón (2000)). Extensions to longer horizons are discussed in (Quevedo, Goodwin, and De Doná (2004) and Quevedo, Müller, and Goodwin (2007)).

5.6. The spectra of uncertainty

We return to the general formulation described in Sections 5.2 and 5.3. Unfortunately, the core stability result assumes no uncertainty (i.e., no disturbances or modelling error).

If uncertainty is present, the equivalence between open-loop and feedback control disappears and the proven stability properties of deterministic model predictive control are lost. Thus it is no longer true that the solution to an open-loop optimal control problem (modified to compensate for its finite horizon) provides optimal control of the uncertain system. We could envisage a "feedback" solution to account for uncertainty; however, an optimal control problem that provides the optimal "feedback" solution would be impossibly complex. Hence, as in adaptive control, 'smart' non-optimal solutions have to be devised. What is often done in practice is to obtain model predictive control for the *nominal* system, i.e., to ignore uncertainty in computing the on-line control action. This can give satisfactory control (but is not guaranteed to do so). To see what might happen, consider the simple case when the state is measured but a disturbance, w, enters additively; the system is then described by

$$x^+ = f(x, u) + w \tag{66}$$

Since now $x^+ = f(x, \kappa_N(x)) + w$ rather than $x^+ = f(x, \kappa_N(x))$, the evolution equation for the value function $V_N^0(\cdot)$ (of the nominal control problem) satisfies

$$V_N^0(x^+) = V_N^0(x) - \ell(x, \kappa_N(x)) + \Delta(x, w) \tag{67}$$

The extra term, $\Delta(x, w) := V_N^0(f(x, \kappa_N(x)) + w) - V_N^0(f(x, \kappa_N(x)))$, may well exceed $\ell(x, \kappa_N(x))$ in magnitude so that a decrease of the candidate Lyapunov function is no longer ensured. Also, recursive feasibility is no longer guaranteed.

To overcome these features of nominal MPC various schemes have been proposed. One proposal, called *tube* model predictive control (Rawlings & Mayne, 2009), uses nominal MPC to determine a nominal trajectory from the current set point to the next set point and local feedback to confine the trajectories of the uncertain system to remain in a specified neighbourhood of the nominal trajectory. If the system $f(\cdot)$ is linear and if $z(i)$ and $v(i)$ are the state and control of the nominal system at time i, the control $u(i)$ applied to the plant is $u(i) = v(i) + K(x(i) - z(i))$ where $x(i)$ is the current state of the plant. If the disturbance, w, is bounded, a bounded set S may be computed such that the state $x(i)$ of the plant satisfies $x(i) \in z(i) + S$ for all i and all possible disturbance sequences. The state $z(i)$ of the nominal system converges to the set point x^* and the state $x(i)$ of the uncertain system converges to the set $x^* + S$; once the state $x(i)$ enters the set $x^* + S$, it remains there. With this knowledge, nominal MPC may be designed

to ensure that the uncertain system satisfies all constraints. If the state is not directly measured, as is commonly the case, a similar procedure is used to control the state estimator. The latter can be viewed as another "uncertain system" with measured state.

5.7. Quantized control

The stability results described above assume the control u lies in, say, $\mathbb{U}$ where the input constraint set $\mathbb{U}$ is a convex subset of, say, $\mathbb{R}^m$. In switching electronics, $\mathbb{U}$ is typically a finite subset of $\mathbb{R}^m$, e.g. $\mathbb{U} = \{u_1, u_2, \ldots, u_m\}$ is the set of voltages, say, that may be generated by the power electronics. A *finite alphabet* $\mathbb{U}$ raises new problems regarding a proof of stability. Some of these problems are discussed below.

6. Certificates of stability

6.1. General comments

It is desirable, but not always possible, to imbue a control law with a "certificate of stability".

In the context of model predictive control, stability can be achieved by adding to the optimal control problem a terminal cost function that is a *global* Control Lyapunov Function or by adding a terminal cost function that is merely a *local* Control Lyapunov Function provided that a terminal constraint is also added such that the local Control Lyapunov Function is valid within the terminal constraint set. This, in turn, raises the issue of "feasibility", i.e., the ability to steer the system from its initial state into the terminal constraint set. This is where a longer horizon can be useful since it offers greater flexibility (i.e., more control moves) to reach the terminal set.

Several special cases facilitate the search for a Control Lyapunov Function. Two such cases are discussed below.

 (i) When the B matrix in the system description is invertible. The key point about this case is that it is always possible to steer any initial state lying sufficiently close to the target state x^* to a point "closer" to the target state (even in one step). Hence, in this case, there exists a wide range of *local* Control Lyapunov Functions, such as the function $|x - x^*|$ used in some switching electronic applications. In this case, the Control Lyapunov Function is local because the control constraint restricts the range of states that can be moved "closer" to the target state.
(ii) When the system is open loop stable. The key point about this case is that one can choose the Control Lyapunov Function (CLF) to be the function $V_f(x) := (1/2)(x - x^*)'P(x - x^*)$ where x^* is the target state and P is the solution of the Lyapunov equation

$$P = A^T P A + \Omega \tag{68}$$

where Ω is any positive definite symmetric matrix. With this choice for $V_f(\cdot)$, the control $u = u^*$, which steers the system to x^*, causes a reduction in the CLF and any control that minimizes $V_f(x^*)$, $x^+ = Ax + Bu$, will decrease the CLF more and steer the system to x^* even more quickly. This CLF is global and this makes it preferable to the local CLF discussed in (i). Invertibility of B is also not required in this case.

Obtaining a control by minimizing $V_f(x^+)$ with respect to u, is actually equivalent to an old form of control in which a Control Lyapunov Function (CLF) is directly employed to obtain a stabilising controller. However, MPC provides extra freedom. For example, a stabilising controller may also be obtained by employing the cost $V_1(x, u) := \ell(x, u) + V_f(Ax + Bu)$ in place of

$V_1(x, u) := V_f(Ax + Bu)$. As before, $V_f(\cdot)$ should be a CLF. The function $\ell(\cdot)$, which should satisfy some simple conditions, may be used to improve performance if $V_f(\cdot)$ is chosen appropriately. Larger horizons would provide even more flexibility.

6.2. Quantization

Quantization introduces an extra layer of difficulty over those described above. For example, with finite alphabet control it is not a-priori obvious that one has the flexibility to steer the state to a desired target x^* that is an equilibrium state in the sense that there exists a control u^* satisfying $x^* = Ax^* + Bu^*$ even if B is invertible. Difficulty arises if the control u^* does not lie in the finite alphabet. This problem requires a more detailed analysis.

One option would be to relax the problem by ignoring the discrete nature of $\mathbb{U}$, i.e., $\mathbb{U}$ is replaced in the optimal control problem by $\mathbb{V}$ which is defined to be the convex hull of $\mathbb{U}$ yielding a control u. The control actually applied to the plant is then $u_{\text{true}} = Q(u)$ where Q is a generalized quantizer. The quantizer noise $q := u_{\text{true}} - u$ is bounded so that the plant, if it is linear, is now described by

$$x^+ = Ax + Bu_{\text{true}} + Bq \tag{69}$$

and is an uncertain system with bounded additive disturbance $w = Bq$. This can be treated by using techniques from the emerging theory of robust model predictive control – see Rawlings and Mayne (2009), Løvaas, Serón, and Goodwin (2008), Løvaas, Serón, and Goodwin (2009), Løvaas, Serón, and Goodwin (2010).

6.3. Fusion control

It has been suggested above that one way to treat quantization is to transform the optimization problem into one with unquantized control and additive bounded noise. Of course, noise comes in different "flavours". Hence, there may be value in combining some of the ideas used in Section 3 with model predictive control. We term such strategies "fusion control" since the goal is to fuse modern and traditional ideas.

6.4. The SynRM revisited

The voltage and torque equations for a three-phase synchronous reluctance motor in the rotating DQ reference frame are given in Section 2. If the state x for the current loop is defined to be the vector (i_d, i_q), then the system satisfies:

$$\dot{x} = \bar{A}(\omega_0)x + \bar{B}u$$
$$y = c(x)$$

where

$$\bar{A} := \begin{bmatrix} -\alpha_1 & \beta_1(\omega_0) \\ -\beta_2(\omega_0) & -\alpha_2 \end{bmatrix}, \quad \bar{B} := \begin{bmatrix} 1/L_1 & 0 \\ 0 & 1/L_2 \end{bmatrix} \tag{70}$$

and

$$c(x) := \frac{3}{2}\frac{p}{}(L_d - L_q)x_1 x_2 \tag{71}$$

where $\alpha_1 := R_s/L_d$, $\alpha_2 := R_s/L_q$, $\beta_1(\omega_0) := (L_d/L_q)\omega_0$, $\beta_2(\omega_0) := (L_q/L_d)\omega_0$, u denotes the voltage vector (v_d, v_q), ω_0 is the 'electrical' angular velocity, y is the output torque and p is the number of pole pairs in the motor. The open loop characteristic polynomial is

$$\phi(s) = s^2 + (\alpha_1 + \alpha_2)s + \alpha_1\alpha_2 + \omega_0^2 \tag{72}$$

This characteristic polynomial is lightly damped if ω_0 is large. The outer loop of the speed control system provides a reference current x^* for an inner loop; x_1^* is constant at a value that

provides maximum flux while x_2^* is varied by the outer loop to achieve the desired angular velocity ω_0^*. The discrete-time model for the inner loop corresponding to a sampling period of Δ_s seconds is:

$$x^+ = Ax + Bu \tag{73}$$

where $A := \exp(\bar{A}\Delta_s)$ and $B := \int_0^{\Delta_s} \exp(\bar{A}t)\bar{B}dt$. This translates the problem into a form where one could use MPC. However, the core problem is the finite alphabet nature of the control. Hence MPC with horizon length N requires choosing, via optimization, a control sequence lying in $\mathbb{U}^N$. This is a difficult problem if N is large. If we use a horizon length $N = 1$, then the problem becomes much simpler as discussed in Section 5.5.4. Moreover, for this particular problem, $\bar{B}$ and hence B, are nonsingular and A is stable. Hence, the ideas discussed in Section 6.1 (i) and (ii) are potentially useful.

7. Challenges and opportunities

7.1. Horizon length

Much of the literature on MPC for switching electronic applications uses, for computational reasons, a horizon length N of unity although there are a few exceptions (Cortés et al., 2008; Geyer, Papafotiou, & Morari, 2009). As we have shown in Section 6.2, it is possible to establish closed loop stability with $N = 1$, e.g., if the system being controlled is invertible in one step or is open loop stable which is the case in some applications. There is a need to investigate whether significantly better performance can be obtained with longer horizons together with suitable choice of the stage cost $\ell(\cdot)$, state constraint, and terminal cost. If a (global) control Lyapunov is available, as is often the case, a terminal constraint is not required. Indeed much of the power of MPC arises from its flexibility in choice of cost function and from its ability to handle hard constraints. Longer horizons may help with performance objectives such as reduction of switching frequency (Geyer et al., 2009) although there is inevitably a trade-off between switching losses and harmonic minimization. It would also be helpful to know under what conditions a horizon length of unity yields good performance.

7.2. Quantization effects

There appear to be two distinct possibilities in MPC for handling the quantization that is induced by the switching converters. One, that seems to be preferred in the current literature, is to pose the optimal control problems as minimizing a cost subject to the constraint $\mathbf{u} \in \mathbb{U}^N$ where $\mathbb{U}$ is the discrete set specifying permissible switched voltages. This approach requires solution of an integer program. The second alternative, also discussed above, is to perform the minimization over $\mathbb{V}^N$ where $\mathbb{V}$ is the convex hull of $\mathbb{U}$. The resultant optimal u is then quantised and the nearest neighbour to u applied to the plant; alternatively PWM or SVF modulation may be employed as is done when PI control is used. The relaxed problem is simpler, being a conventional quadratic or nonlinear programme. This permits a traditional analysis of closed loop stability. It would be interesting to compare the performances of these two approaches. Also, the potential advantages of using feedback around the quantizer to modify the frequency spectrum of the quantization errors should be explored.

7.3. Robustness

Existing design techniques for unconstrained control problems permit a wide range of robustness issues such as undermodelling, unknown parameters, unknown states, the effect of disturbances to be addressed. Unfortunately, the same is not true for MPC since, as pointed out above, the solution to the open loop optimal control problem solved online is not equivalent to the feedback solution. A consequence is that *nominal* MPC, which ignores uncertainty and is widely used, may have poor robustness properties. Current research is searching for modifications to nominal MPC that ensure robustness. Some proposals have been made for the case when the uncertainty takes the form of an unknown, but bounded, disturbance and also when the state has to be estimated. Recent work on unmodelled dynamics is given in (Løvaas et al., 2008; Løvaas et al., 2009; Løvaas et al., 2010; Maciejowski, 2002; Matsuo & Lipo, 1994; Mayne, Rawlings, Rao, & Scokaert, 2000; Miranda, Cortés, & Rodríguez, 2009; Mohan, Underland, & Robbins, 1995; Mulle, Ammann, & Rees, 2005; Nešić & Grüne, 2006; Papafotiou, Geyer, & Morari, 2007; Papafotiou, Kley, Papadopoulos, Bohren, & Morari, 2009; Perantzakis, Xepapas, Papathanassiou, & Manias, 2005; Qin & Badgwell, 2003; Quevedo, Aguilera, Pérez, & Cortés, 2010; Quevedo & Nešić, in press) .

7.4. Control architecture

In classical control several different architectures have been employed to good effect. One of these is the multi-degree-of-freedom controller architecture as described in Section 3.6. It would be interesting to know if MPC would benefit from more complex architectures Bemporad (1998) than the single loop that is currently employed. A related question is the use of 'inner' and 'outer' loops. In some applications, MPC is used for an inner current or torque loop and a conventional controller for an outer speed loop. This raises the question as to whether or not it would be advantageous to dispense with the inner loop and use a single model predictive controller for the outer loop? Another alternative would be to employ model predictive controllers in both the inner and outer loop.

7.5. Cost function

The cost function for power electronic applications typically has a "standard" form which assigns penalty coefficients to each component of the output error. This is somewhat arbitrary and subjective process. Development of a unified approach to cost function design would be beneficial. Variable or adaptive cost functions that achieve best performance under varying operating conditions and alternative design requirements would be useful.

8. Conclusion

This paper has given a tutorial overview of the application of control to switching electronic systems. We have also commented on issues that arise when these techniques are applied to switched systems and we have raised a number of open problems and challenges.

Acknowledgment

References

Aguilera, R. P., Quevedo, D. E., Summers, T. J., & Lezana, P. (2008). Predictive control algorithm robustness for achieving fault tolerance in multicell converters. *Proc. 34th Annual Conf. IEEE Ind. Electron. Soc. (IECON'08)* (pp. 3302–3308).

Bemporad, A. (1998). Reference governor for constrained nonlinear systems. *IEEE Transactions. Automat. Control, 43*(3), 415–419.

Camacho, E. F., & Bordons, C. (1999). *Model predictive control.* New York, NY: Springer-Verlag.

Coates, C. E., Platt, D., & Gosbel, V. J. (2001, October). Performance evaluation of a nine-phase synchronous reluctance drive. In *Proceedings of IEEE—IAS Annual Meeting, Vol. 3* (pp. 2041–2047).

Cortés, P., Kazmierowski, M. P., Kennel, R. M., Quevedo, D. E., & Rodríguez, J. (2008, December). Predictive control in power electronics and drives. *IEEE Transactions on Industrial Electronics, 55*, 4312–4324.

Cortés, P., Rodríguez, J., Quevedo, D. E., & Silva, C. (2008, March). Predictive current control strategy with imposed load current spectrum. *IEEE Transactions on Power Electronics, 23*, 612–618.

Cortés, P., Ortiz, G., Yuz, J. I., Rodríguez, J., Vázquez, S., & Franquelo, L. G. (2009, June). Model predictive control of an inverter with output LC-filter for UPS applications. *IEEE Transactions on Industrial Electronics, 56*, 1875–1883.

De Doná, J. A., Goodwin, G. C., & Serón, M. M. (2000). Anti-windup and model predictive control: Reflections and connections. *European Journal of Control, 6*(5), 467–477.

Gersho, A., & Gray, R. M. (1992). *Vector quantization and signal compression*. Boston, MA: Kluwer Academic.

Geyer, T., Papafotiou, G., & Morari, M. (2009, June). Model predictive direct torque control. Part I. Concept, algorithm and analysis. *IEEE Transactions on Industrial Electronics, 56*, 1894–1905.

Goodwin, G. C., Graebe, S. E., & Salgado, M. (1997). *Principles of control system design*. Englewood Cliffs, NJ: Prentice Hall.

Goodwin, G. C., Quevedo, D. E., & McGrath, D. (2003, March). Moving-horizon optimal quantizer for audio signals. *Journal of Audio Engineering Society, 51*, 138–149.

Goodwin, G. C., Quevedo, D. E., & Silva, E. I. (2008, January). Architectures and coder design for networked control systems. *Automatica, 44*, 248–257.

Goodwin, G. C., Serón, M. M., & De Doná, J. A. (2005). *Constrained control & estimation— An optimization perspective*. London: Springer Verlag.

Holmes, D. G., & Lipo, T. A. (2003). *Pulse width modulation for power converters*. Piscataway, NJ: IEEE Press.

Huang, J., & Corzine, K. A. (2006, January). Extended operation of flying capacitor multilevel inverters. *IEEE Transactions on Power Electronics, 21*, 140–147.

Kazmierowski, M. P., Krishnan, R., & Blaabjerg, F. (2002). *Control in power electronics*. Academic Press.

Kouro, S., Cortés, P., Vargas, R., Ammann, U., & Rodríguez, J. (2009, June). Model predictive control—A simple and powerful method to control power converters. *IEEE Transactions on Industrial Electronics, 56*, 1826–1838.

Lezana, P., Aguilera, R. P., & Quevedo, D. E. (2009, June). Model predictive control of an asymmetric flying capacitor converter. *IEEE Transactions on Industrial Electronics, 56*, 1839–1846.

Lipo, T. A. (1991). Synchronous reluctance machines—A viable alternative for AC drives? *Electric Machines and Power Systems, 19*, 659–671.

Linder, A., & Kennel, R. (2005). Model predictive control for electrical drives. *Proc. IEEE Power Electronics Specialists Conference (PESC)* (pp. 1793–1799).

Løvaas, C., Serón, M. M., & Goodwin, G. C. (2008). Robust output feedback model predictive control for systems with unstructured uncertainty. *Automatica, 44*, 1933–1943.

Løvaas, C., Serón, M. M., & Goodwin, G. C. (2009). Inverse minimax optimality of model predictive control policies. *Systems & Control Letters, 58*, 31–38.

Løvaas, C., Serón, M. M., & Goodwin, G. C. (2010). Robust output feedback MPC with integral action. *IEEE Trans. Automat. Contr., 55*(7), 1531–1543.

Maciejowski, J. M. (2002). *Predictive Control with Constraints*. Englewood Cliffs, N.J. Prentice-Hall.

Matsuo, T., & Lipo, T. A. (1994). Rotor design optimization of a synchronous reluctance machine. *IEEE Transactions on Energy Conversion, 9*(2), 359–365.

Mayne, D. Q., Rawlings, J. B., Rao, C. V., & Scokaert, P. O. M. (2000, June). Constrained model predictive control: Optimality and stability. *Automatica, 36*, 789–814.

Miranda, H., Cortés, P., Yuz, J. I., & Rodríguez, J. (2009, June). Predictive torque control of induction machines based on state-space models. *IEEE Transactions on Industrial Electronics, 56*, 1916–1924.

Mohan, N., Underland, T. M., & Robbins, W. P. (1995). *Power Electronics*. Hoboken, NJ: Wiley.

Muller, S., Ammann, U., & Rees, S. (2005, December). New time-discrete modulation scheme for matrix converters. *IEEE Transactions on Industrial Electronics, 52*, 1607–1615.

Nešić, D., & Grüne, L. (2006). A receding horizon control approach to sampled-data implementation of continuous-time controllers. *Systems & Control Letters, 55*, 660–672.

Papafotiou, G., Geyer, T., & Morari, M. (2007). A hybrid model predictive control approach to the direct control problem of induction motors. *International Journal of Robust and Nonlinear Control, 17*(17), 1572–1589.

Papafotiou, G., Kley, J., Papadopoulos, K. G., Bohren, P., & Morari, M. (2009, June). Model predictive direct torque control. Part II. Implementation and experimental evaluation. *IEEE Transactions on Industrial Electronics, 56*, 1906–1915.

Perantzakis, G., Xepapas, F., & Manias, S. N. (2005, September). Efficient predictive control technique for multilevel voltage source inverters. *Proc. Eur. Conf. Power Electron. Appl.*.

Perantzakis, G., Xepapas, F., Papathanassiou, S., & Manias, S. N. (2005). A predictive current control technique for three-level NPC voltage source inverters. *Proc. IEEE Power Electronics Specialists Conference (PESC)* (pp. 1241–1246).

Qin, S. J., & Badgwell, T. A. (2003). A survey of industrial model predictive control technology. *Control Engineering Practice, 11*, 733–764.

Quevedo, D. E., Aguilera, R. P., Pérez, M. A., & Cortés, P. (2010). Finite control set MPC of an AFE rectifier with dynamic references. *Proc. IEEE Conf. on Industrial Technology*.

Quevedo, D. E., & Goodwin, G. C. (2005, March). Multistep optimal analog-to-digital conversion. *IEEE Transactions on Circuits Systems I, 52*, 503–515.

Quevedo, D. E., Goodwin, G. C., & De Doná, J. A. (2004, March). Finite constraint set receding horizon quadratic control. *International Journal of Robust and Nonlinear Control, 14*, 355–377.

Quevedo, D. E., Müller, C., & Goodwin, G. C. (2007, May). Conditions for optimality of naïve quantized finite horizon control. *International Journal of Control, 80*, 706–720.

Quevedo, D. E. & Nešić, D. (in press). Input-to-state stability of packetized predictive control over unreliable networks affected by packet-dropouts, IEEE Transactions on Automatic Control

Rawlings, J. B., & Mayne, D. Q. (2009). *Model Predictive Control: Theory and Design*. Madison, WI: Nob Hill Publishing.

Rodríguez, J. R., Pontt, J., Silva, C., Correa, P., Lezana, P., & Cortés, P. (2007, February). Predictive current control of a voltage source inverter. *IEEE Transactions on Industrial Electronics, 54*, 495–503.

Silva, E. I., Goodwin, G. C., & Quevedo, D. E. (2010, February). Control system design subject to SNR constraints. *Automatica, 46*, 428–436.

Vargas, R., Cortés, P., Ammann, U., Rodríguez, J., & Pontt, J. (2007, October). Predictive control of a three-phase neutral point-clamped inverter. *IEEE Transactions on Industrial Electronics, 54*, 2697–2705.

Vas, P. (2003). *Sensorless Vector and Direct Torque Control*. Oxford university Press.

Xu, L., Xu, X., Lipo, T. A., & Novotny, D. W. (1991). Vector control of a synchronous reluctance motor including saturation and iron loss. *IEEE Transactions on Industry Applications, 27*(5), 977–985.

Graham C. Goodwin Graham Goodwin obtained a B.Sc. (physics), B.E. (electrical engineering), and Ph.D. from the University of New South Wales. He is currently Professor Laureate of electrical engineering at the University of Newcastle, Australia, and is director of an Australian Research Council Centre of Excellence for Complex Dynamic Systems and Control. He holds Honorary Doctorates from Lund Institute of Technology, Sweden, and the Technion Israel. He is the co-author of eight books, four edited books, and many technical papers. Graham is the recipient of Control Systems Society 1999 Hendrik Bode Lecture Prize, a Best Paper award by IEEE Transactions on Automatic Control, a Best Paper award by Asian Journal of Control, and 2 Best Engineering Text Book awards from the International Federation of Automatic Control in 1984 and 2005. In 2008 he received the Quazza Medal from the International Federation of Automatic Control. He is a Fellow of IEEE; an Honorary Fellow of Institute of Engineers, Australia; a Fellow of the International Federation of Automatic Control; a Fellow of the Australian Academy of Science; a Fellow of the Australian Academy of Technology, Science and Engineering; a Member of the International Statistical Institute; a Fellow of the Royal Society, London; and a Foreign Member of the Royal Swedish Academy of Sciences.

David Q. Mayne David Mayne received the B.Sc. and M.Sc. degrees from the University of the Witwatersrand, the Ph.D. and D.Sc. degrees from the University of London, and the degree of Doctor of Technology, honoris causa, from the University of Lund, Sweden. He has held posts at the University of the Witwatersrand, the British Thomson Houston Company, University of California, Davis and Imperial College London where he is now Senior Research Fellow. His research interests include optimization, optimization based design, nonlinear control and model predictive control.

Keng-Yuan Chen Keng-Yuan Chen received the B.S. degree from the Department of Electrical and Control Engineering, National Chiao-Tung University, Taiwan, in 2003, and the M.S. degree from the Department of Electrical and Control Engineering, National Chiao-Tung University, Taiwan, in 2005. She is currently a Ph.D. candidate in the Department of Electrical and Control Engineering, National Chiao-Tung University, Taiwan, ROC. Her main research interests cover digital signal processing and class-d amplification.

Colin Coates Colin Coates received both the B.Math–B.E. degree in electrical engineering and Ph.D. from the University of Wollongong, Australia, in 1993 and 2002 respectively. He has over 10 years industry experience having worked for both BHP Steel (automation and drives) and Zener Electric (power electronics design). He joined the University of Newcastle, Australia, in 1999. His research interests include low voltage distributed generation, wind turbine control and electric drives.

Galina Mirzaeva Galina Mirzaeva received M.E. (1990) and Ph.D. (1997) from the South Ural State University, Russia. In 1993–1998 she worked with the Makeev National Rocket Centre, Russia. In 2004–2009 she was a Research Academic with CRC Mining at the University of Newcastle, Australia. Since 2009 she is a Senior Lecturer with School of Electrical Engineering and Computer Science of the same University. Her research interests include control and dynamic performance of AC and DC machines and various aspects of power electronics and autonomous power generation. She is a member of Industrial Drives Committee and the Chair of Mining Industry Committee of the IEEE Industry Applications Society.

Daniel Quevedo Daniel E. Quevedo received Ingeniero Civil Electrónico and Magister en Ingeniería Electrónica degrees from the Universidad Técnica Federico Santa María, Valparaíso, Chile, in 2000. In 2005, he received the Ph.D. degree from The University of Newcastle, Australia, where he is currently a research academic. He has been a visiting researcher at ETH Zürich, Switzerland, at Uppsala University, Sweden, at The University of Melbourne, Australia, at Aalborg University, Denmark, at Kyoto University, Japan, and at KTH Stockholm, Sweden. Dr. Quevedo was supported by a full scholarship from the alumni association during his time at the Universidad Técnica Federico Santa María and received several university-wide prizes upon graduating. He received the IEEE Conference on Decision and Control Best Student Paper Award in 2003 and was also a finalist in 2002. In 2009, he was awarded an Australian Research Fellowship. His research interests cover several areas of automatic control, signal processing, communications, and power electronics.